DOI:
10.1016/j.neurobiolaging.2018.06.015

Document Version
Peer reviewed version

Accepted Manuscript

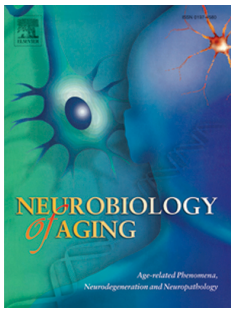

ALS-associated missense and nonsense *TBK1* mutations can both cause loss of kinase function

Martina de Majo, Simon D. Topp, Bradley N. Smith, Agnes L. Nishimura, Han-Jou Chen, Athina Soragia-Gkazi, Jack Miller, Chun Hao Wong, Caroline Vance, Frank Baas, Anneloor LMA. ten Asbroek, Kevin P. Kenna, Nicola Ticozzi, Alberto Garcia Redondo, Jesús Esteban-Pérez, Cinzia Tiloca, Federico Verde, Stefano Duga, Karen E. Morrison, Pamela J. Shaw, Janine Kirby, Martin R. Turner, Kevin Talbot, Orla Hardiman, Jonathan D. Glass, Jacqueline de Belleroche, Cinzia Gellera, Antonia Ratti, Ammar Al-Chalabi, Robert H. Brown, Jr., Vincenzo Silani, John E. Landers, Christopher E. Shaw

PII: S0197-4580(18)30219-7

DOI: 10.1016/j.neurobiolaging.2018.06.015

Reference: NBA 10287

To appear in: *Neurobiology of Aging*

Received Date: 18 April 2018

Revised Date: 12 June 2018

Accepted Date: 12 June 2018

Please cite this article as: de Majo, M., Topp, S.D, Smith, B.N, Nishimura, A.L, Chen, H.-J., Soragia-Gkazi, A., Miller, J., Wong, C.H., Vance, C., Baas, F., ten Asbroek, A.L., Kenna, K.P., Ticozzi, N., Redondo, A.G., Esteban-Pérez, J., Tiloca, C., Verde, F., Duga, S., Morrison, K.E., Shaw, P.J., Kirby, J., Turner, M.R., Talbot, K., Hardiman, O., Glass, J.D., de Belleroche, J., Gellera, C., Ratti, A., Al-Chalabi, A., Brown Jr., R.H, Silani, V., Landers, J.E, Shaw, C.E, ALS-associated missense and nonsense *TBK1* mutations can both cause loss of kinase function, *Neurobiology of Aging* (2018), doi: 10.1016/j.neurobiolaging.2018.06.015.

ALS-associated missense and nonsense *TBK1* mutations can both cause loss of kinase function

Authors: Martina de Majo[1], Simon D Topp[1], Bradley N Smith[1], Agnes L Nishimura[1], Han-Jou Chen[1], Athina Soragia-Gkazi[1], Jack Miller[1], Chun Hao Wong[1], Caroline Vance[1], Frank Baas[2], Anneloor LMA ten Asbroek[3], Kevin P. Kenna[4], Nicola Ticozzi[5+6], Alberto Garcia Redondo[7], Jesús Esteban-Pérez[7], Cinzia Tiloca[5+6], Federico Verde[5+6], Stefano Duga[8+9], Karen E. Morrison[10], Pamela J. Shaw[11], Janine Kirby[11], Martin R. Turner[12], Kevin Talbot[12], Orla Hardiman[13], Jonathan D. Glass[14], Jacqueline de Belleroche[15], Cinzia Gellera[16], Antonia Ratti[5+6], Ammar Al-Chalabi[1], Robert H Brown Jr[4], Vincenzo Silani[5+6], John E Landers[4], Christopher E Shaw[1]†

† Corresponding author

Affiliations:

1. United Kingdom Dementia Research Institute, Maurice Wohl Clinical Neuroscience Institute, Institute of Psychiatry, Psychology and Neuroscience, King's College London, 125 Coldharbour Lane, Camberwell, SE5 9NU London, U.K.
2. Department of Clinical Genetics, Leiden University Medical Center, Leiden, The Netherlands.
3. Department of Genome analysis, University of Amsterdam, Academic Medical Centre, PO Box 22700, 1100DE, Amsterdam, The Netherlands.
4. Department of Neurology, University of Massachusetts Medical School, Worcester, Massachusetts 01605, USA.
5. Department of Neurology and Laboratory of Neuroscience, IRCCS Istituto Auxologico Italiano, 20149 Milan, Italy
6. Department of Pathophysiology and Transplantation, 'Dino Ferrari' Centre, Università degli Studi di Milano, 20122 Milan Italy
7. Unidad de ELA, Instituto de Investigación Hospital 12 de Octubre de Madrid, SERMAS, and Centro de Investigación Biomédica en Red de Enfermedades Raras (CIBERER U-723), Madrid, Spain.
8. Department of Biomedical Sciences, Humanitas University, Rozzano - Milan Italy.
9. Humanitas Clinical and Research Center, Via Manzoni 56, 20089 Rozzano - Milan, Italy.
10. University of Southampton, Southampton General Hospital, SO16 6YD, UK.
11. Sheffield Institute for Translational Neuroscience, University of Sheffield, Sheffield, UK.
12. Nuffield Department of Clinical Neurosciences, University of Oxford, Oxford, UK.
13. Academic Unit of Neurology, Trinity Biomedical Sciences Institute, Trinity College Dublin, Dublin, Republic of Ireland.
14. Department of Neurology, Center for Neurodegenerative Disease, Emory University School of Medicine, Atlanta, Georgia 30322, USA.
15. Neurogenetics Group, Division of Brain Sciences, Imperial College London, Hammersmith Hospital Campus, Burlington Danes Building, Du Cane Road, London, W12 0NN.
16. Unit of Genetics of Neurodegenerative and Metabolic Diseases, Fondazione IRCCS Istituto Neurologico 'Carlo Besta', 20133 Milan, Italy.

Corresponding author: Professor Christopher Shaw, Maurice Wohl Clinical Neuroscience Institute, Institute of Psychiatry, Psychology and Neuroscience, King's College London, 125 Coldharbour Lane, Camberwell, SE5 9NU, London, UK. (T) +44 207 848 0974, email: chris.shaw@kcl.ac.uk

Key words: ALS, TBK1, FTD, WES, familial ALS

Abstract

Mutations in TBK1 have been linked to amyotrophic lateral sclerosis (ALS). Some *TBK1* variants are nonsense and are predicted to cause disease through haploinsufficiency, however many other mutations are missense with unknown functional effect. We exome sequenced 699 familial ALS patients and identified 16 *TBK1* novel or extremely rare protein changing variants. We characterised a subset of these: p.G217R, p.R357X and p.C471Y. Here we show that the p.R357X and p.G217R both abolish the ability of TBK1 to phosphorylate two of its kinase targets, IRF3 and OPTN and to undergo phosphorylation. They both inhibit binding to OPTN and the p.G217R, within the TBK1 kinase domain, reduces homodimerisation, essential for TBK1 activation and function. Lastly, we show that the proportion TBK1 that is active (phosphorylated) is reduced in five lymphoblastoid cell lines derived from patients harbouring heterozygous missense or in-frame deletion *TBK1* mutations. We conclude that missense mutations in functional domains of TBK1 impair the binding and phosphorylation of its normal targets, implicating a common loss of function mechanism, analogous to truncation mutations.

1. Introduction

Amyotrophic Lateral Sclerosis (ALS) is an adult onset and progressive neurodegenerative disorder that targets the upper and lower motor neurons in the brain and spinal cord. Death usually occurs within three to five years from the symptom onset and treatment is largely palliative (Morgan and Orrell, 2016). ALS is often associated with cognitive changes linked to mild frontotemporal dementia (FTD) (Gijselinck et al., 2015) and up to 50% of the FTD cases develop signs of motor neuron disease (MND) (van der Zee et al., 2017).

Approximately 10% of ALS cases have a familial history of ALS or FTD (fALS, fALS/FTD) (Tiwari et al., 2005). To date, more than 40 genes have been identified to be associated with ALS through linkage studies, Genome Wide Association Studies (GWAS), Whole Exome Sequencing (WES) and Whole Genome Sequencing (WGS). Four genes account for over 50% of fALS cases: *SOD1, C9ORF72, TARDBP* and *FUS/TLS* in population of European ancestry and most other genes are rare, each accounting for ~1% of the cases (Taylor et al., 2016).

Tank Binding Kinase 1 (*TBK1*, *NAK*, *T2K*) codes for a protein kinase involved in many pathways including the immune response and autophagy (Weidberg and Elazar, 2011). TBK1 is composed by four domains: a kinase domain (KD), responsible for its kinetic activity, an ubiquitin-like domain (ULD), a scaffold dimerization domain (SDD) and a C-terminal domain (CTD), involved in TBK1 association with binding partners such as optineurin (OPTN), an important autophagy receptor (Tu et al., 2013) (Figure 1). TBK1 has been shown to homo-dimerise through a central axis formed by the two SDD domains interacting with each other (Figure 1c). This structure is stabilised by the ULD and the KD that interact with each other and with the SDD axis, forming a globular head that stabilises the whole structure (Tu et al., 2013). The interactions between the ULD, the SDD and their linker region are highly hydrophobic and prevent the homodimer from being dissociated when carrying out its functions. On the other hand, interactions of the KD within this structure are mainly polar (Tu et al., 2013). TBK1 activation has been demonstrated to be a multistep process that begins with the Lys-63-linked polyubiquitination, which is required for Ser172 phosphorylation within the activation loop. This causes a critical change in protein conformation promoting the active position of the C-helix in the SDD domain and facilitating the final step of homo-dimerisation, essential for mature kinase activity (Ma et al., 2012; Tu et al., 2013).

Mutations in *TBK1* have been recently linked with ALS and FTD by two WES/WGS independent studies (Cirulli et al., 2015; Freischmidt et al., 2015). Many ALS-linked *TBK1* mutations generate premature stop

codons, leading to nonsense-mediated mRNA decay and haploinsufficiency that is predicted to impair autophagy (Freischmidt et al., 2016). However, the pathogenicity and mechanism of missense mutations is unclear (Freischmidt et al., 2016). Here we describe 16 novel or extremely rare, potentially deleterious variants in *TBK1*, and demonstrate that missense mutations can lead to a loss of TBK1 kinase activity by either disrupting homodimer formation, phosphorylation of itself and its targets Optineurin (OPTN) and interferon regulatory factor 3 (IRF3), implicating a loss of function pathogenic mechanism.

2. Material and Methods

2.1. Patients and DNA samples

All patients and controls individuals gave full patient consent for research purpose. DNA was extracted from 932 patient samples primarily of European ancestry of which 757 were index cases and 175 were affected relatives. All patients had a diagnosis of ALS following revised El Escorial criteria (Brooks et al., 2000) with at least one family member affected by ALS and/or FTD. Any sample positive for mutations in known ALS genes (eg. *SOD1*, *C9orf72*, *TARDBP*, *FUS*, *PFN1*, *UBQLN2*, *OPTN*, *VCP*, and *ANG*) were excluded from further analysis, resulting in a final cohort of 699 probands. Exome sequence data for 102 FALS cases in this cohort were obtained, with permission, from the dbGAP (database of Genotypes and Phenotypes) repository (National Institutes of Health (NIH) Exome Sequencing of FALS, National Institute of Neurological Disorders and Stroke (NINDS), phs000101. v4.p1, Traynor).

2.2. Exome sequencing and variant analysis

Exomes were captured from the UK samples using the Roche-Nimblegen SeqCap EZ Exome probe library and sequenced on an Illumina HiSeq 2000 producing 100 bp paired-end (PE) reads. All other exomes were provided as FASTQ files, captured with a variety of probe sets and sequenced to produce either 50, 75, or 100 bp Illumina PE reads. Novocraft NovoAlign was used to align the FASTQ files to the hg19 human reference, variants were called with SAMtools v1.1mpileup then normalised with bcftools v1.1 norm. Individual variant call files (VCF) were filtered by the following criteria: DP≥10, QUAL>20, GQ≥50, and MQ≥50 then merged to a single cohort VCF. Common ancestry between samples was taken from existing familial annotation where available and also deduced from inheritance by descent (IBD) analysis in vcftools (Yang et al., 2011) and King (Manichaikul et al., 2010), using only variant positions covered to a depth >10 in >85% of FALS cases, and recoding all missing data to a heterozygous reference genotype (0/0). Functional annotation, pathogenicity predictions, AdaBoost (ADA) & Random Forest (RF) splicing predictions (Jian et al., 2014) and matches to 1000 genomes were added with table_annovar.pl (Wang et al.,

2010), whereas all other annotations including variant frequencies in Exome Sequencing Project (ESP, http://evs.gs.washington.edu/EVS), Exome Aggregation Consortium (ExAC, http://exac.broadinstitute.org) and UK10K (www.uk10k.org), were added via custom perl scripts. Variants were removed if they had a carrier frequency of greater than 1 in 20,000 in the Non-Finnish European (NFE) subset of ExAC (MAF>0.0025%) or were predicted benign by at least 15 of the 20 pathogenicity prediction algorithms. Synonymous and intronic variants were assessed by NetGene2 and GeneSplicer and excluded if no changes in scores were observed compared to the reference allele at locations matching to known Refseq acceptor or donor splice sites. 5' and 3' UTR variants were excluded from consideration in this analysis. To assess the relative abundance of *TBK1* variants in our cohort compared to ExAC, a burden test (Fisher's Exact, two tailed) was performed between the number of FALS and ExAC NFE variants remaining after annotation and filtering by the above criteria.

2.3. Plasmid and Cloning

HA-tagged *TBK1* wild type (WT) and FLAG-tagged *OPTN* pCMV3 expression vectors were purchased from Creative Biogene Biotechnology. Single amino acid changes (p.G217R, p.R357X, p.C471Y) were introduced in HA-tagged *TBK1* WT by site direct mutagenesis using Q5® Site-Directed Mutagenesis Kit according to manufacturer's protocol (New England Biolabs). All constructs were verified by Sanger sequencing.

2.4. Antibodies

Mouse and rabbit HA-tag monoclonal antibodies were used at a dilution of 1/1000 for western blot and 1/500 for immunocytochemistry (ICC) (cat no. 2367 and 3724, Cell Signaling Technology). Rabbit anti-TBK1 monoclonal antibody was used at a dilution of 1/1000 (cat no ab40676, Abcam). Rabbit anti-phospho-TBK1 (S172) monoclonal antibody was used at a dilution of 1/500 for western blot and 1/50 for ICC (cat no. 5483, Cell Signaling Technology). Rabbit anti- Interferon regulatory factor 3 (IRF3) polyclonal antibody was used at a dilution of 1/200 (cat no. A022993, Bioassay Technology Laboratory). Rabbit anti-phospho-IRF-3 (Ser396) monoclonal antibody was used at a dilution of 1/200 for ICC and western blot (Cat no. ab76493, Abcam). Mouse anti- DYKDDDDK (FLAG) monoclonal antibody was used at a dilution of 1/3000 (Cat no. TA5001, Origene). Mouse anti- Glyceraldehyde 3-phosphate dehydrogenase (GAPDH) monoclonal antibody was used at a dilution of 1/6000 (Cat no. G8795, Sigma-Aldrich).

2.5. Culture of lymphoblastoid cell lines

Lymphoblastoid cell lines (LCLs) derived from FALS patients and healthy controls were obtained from the European Collection of Authenticated Cell Cultures (ECACC). LCLs were grown in RPMI media (Gibco, Life Technologies) complemented with 10% FBS (Fetal Bovine Serum, Life Technolgies), 5% PenStrep (penicillin 100 U/ml and streptomicin 100 U/ml, Life Technologies) and 5% L-Glutamine (Life Technologies). These cells grow in suspension and were, therefore, kept in upright T25 flasks (Nunc, Life Technologies) in a water-jacketed 5% CO_2 incubator.

2.6. Culture and Transfection of HEK293T cells

HEK293T cells were cultured in Dulbecco's modified Eagle's medium (DMEM) with 10% Foetal Bovine Serum (FBS), 5% PenStrep (penicillin 100 U/ml and streptomicin 100 U/ml), 5% Glutamine (Life Technologies) in a water-jacketed 5% CO_2 incubator. For western blot, native gel and immunoprecipitation analysis cells were plated in six-well plates (Life Technologies) and transfected with 1μg of plasmid DNA, 2 μl of Lipofectamine 2000 (Life Technologies) and 100 μl of OPTIMEM (Life Technologies) per well according to manufacturer's instructions. For immunofluorescence (ICC), HEK293T cells were plated in 24 well-plates (Life Technologies) on thirteen-mm-diameter coverslips (VWR) pre-coated with poly-D-lysine (Sigma-Aldrich) and transfected with 250 ng of plasmid DNA, 0.5 μl of Lipofectamine 2000 (Life Technologies) and 25 μl of OPTIMEM (Life Technologies) per well, according to manufacturer's instructions. Cells were processed for western blot, immunoprecipitation, native gel or ICC after 48 hours of transient transfection.

2.7. RNA extraction and RT-PCR

Total RNA was extracted using RNeasy Mini Kit (Qiagen) according to manufacturer's protocol. The extracted RNA was used as a template for the synthesis of complementary DNA (cDNA) through reverse transcription, using SuperScript® III Reverse Transcriptase (Life Technologies) following manufacturer's protocol. Oligo dT were used to synthesise cDNA. cDNA was amplified using the PCR primers ATGCAGAGCACTTCTAATCATCTGTGGC and CTAAAGACAGTCAACGTTGCGAAG and Sanger sequenced using the sequencing primers TTGAAGGGCCTCGTAGGAAT and TCAGCCATCGTATCCCCTTT.

2.8. Immunocytochemistry (ICC)

48 hours after transfection cells were fixed with 4% PFA at room temperature for fifteen minutes, permeabilised with 0.2% Triton-X-100 for 30 minutes and blocked with 5% Goat Serum (Sigma) for one hour at room temperature. Samples were incubated with primary antibody (anti-HA tag 1/500, anti-pTBK1

1/50, anti-pIRF3 1/200) in 1% Goat Serum overnight at 4 °C. Fluorescent tagged secondary antibodies (Alexa Fluor 488 Goat IgG Antibody, Alexa Fluor 568 Goat IgG Antibody, 1/500 Life Technologies) were used for fluorescence detection according to manufacturer's instructions. As a negative control samples were incubated with primary antibody only or secondary antibody only (data not shown). DAPI (4', 6-diamidino-2-phenylindole) was used to detect the nuclei. Coverslips were mounted on microscope slides (Thermo Scientific) and imaged using Leica confocal SP5 microscope (Leica).

2.9. Western blot analysis

HEK293T cells were harvested 48 hours after transfection in Phosphate-Buffer Saline (PBS, Severn Biotech LTD) complemented with phosphatase inhibitors (PhoSTOP, Roche) and proteinase inhibitors (COMPLETE, Roche). LCLs were harvested collecting cells in 15ml tube (Falcon), centrifuged to form a pellet and resuspended in PBS complemented with phosphatase inhibitors (PhoSTOP, Roche) and proteinase inhibitors (COMPLETE, Roche). Cells were then lysed and processed as previously described (Scotter et al., 2014). Membrane imaging was conducted using goat anti-rabbit, and anti-mouse IgG (H+L) DyLight 680 Conjugate (cat. no. 35568 and 35521, Thermo Life Sciences) and a LI-COR Odyssey or using horseradish peroxidase (HRP) secondary antibodies for mouse (Millipore, 12-349) or rabbit (Millipore, 12-348) and developed through Enhanced chemiluminescence (ECL) system using Medical Film Processor SRX-101A (Konica Minolta). Western blot quantification was performed using the image analysis software, ImageJ (http://imagej.nih.gov/ij/ (Schindelin et al., 2012)).

2.10. Native gel electrophoresis

Cells were harvested in PBS complemented with phosphatase inhibitors and proteinase inhibitors. Samples were then processed using NativePAGE™ Novex® Bis-Tris Gel System according to manufacturer's protocol. Protein were transferred on a polyvinylidene difluoride (PVDF) membrane, previously activated in methanol, using wet transfer system (300mA one hour). The membrane was then incubated in 8% acetic acid, air dried and washed in methanol. A blocking solution of 5% bovine serum albumin (BSA) was used to block the membrane for 30 minutes prior incubation with 1% BSA and primary antibody (anti-HA tag 1/200) at 4°C overnight. Membrane imaging was conducted using goat anti-rabbit, and anti-mouse IgG (H+L) DyLight 680 Conjugate (cat. no. 35568 and 35521, Thermo Life Sciences) and a LI-COR Odyssey.

2.11. Cotransfection IP assay

Cells were transfected with *TBK1* WT and mutant plasmids together with *OPTN* WT plasmids. Additional controls untransfected, and transfected with either *TBK1* WT or *OPTN* WT only were used. After 48 hours

cell were harvested in immunoprecipitation (IP) buffer (50 mM tris (pH 7.4), 150 mM NaCl, 1% Triton X-100, and 100 mM$CaCl_2$ with protease and phosphatase inhibitors). Lysates were partly harvested and diluted in loading buffer complemented with 250 mM 1,4-Dithiothreitol (DTT, Thermo Scientific). The lysates were pre cleaned through incubation with Dynabeads ® Protein G for Immunoprecipitation (Life Technologies) at 4°C for two hours. The beads were then discarded and the lysate incubated with Dynabeads ® Protein G and anti-HA tag antibody (1/100) at room temperature for two hours. As an additional negative control two samples transfected with *OPTN* WT only or *TBK1* WT only were incubated with beads and no antibody, to reveal any unspecific binding. The beads were separated from the flow-through (FT) through magnetic separation and washed with IP buffer six times before elution in loading buffer complemented with DTT. Lysates and IP fractions were analysed by western blot.

2.12. Phosphatase assay

Cells were transfected with *TBK1* WT and mutant plasmids together with *OPTN* WT plasmids. Additional controls untransfected or transfected with either *TBK1* WT or *OPTN* WT only were used. After 48 hour transfected cells were harvested in RIPA buffer (50 mM Tris pH 8.0, 150 mM NaCl, 1% NP-40, 0.5% sodium deoxycholate, 0.1% sodium dodecyl sulphate with protease inhibitor) and sonicated for ten seconds. Six µg of protein per sample was added to 3µl of CIP buffer (100 mM NaCl, 50 mM Tris-HCl, 10 mM $MgCl_2$, 1 mM dithiothreitol, pH to 7.9 at 25°C) and 3µl of alkaline phosphatase (Roche) were added to the phosphatase positive samples, according to Abcam protein dephosphorylation protocol (http://www.abcam.com/protocols/protein-dephosphorylation-protocol). All the samples were incubated for 30 minutes at 37 °C and ran on NuPAGE Novex 3-8% Tris-Acetate Midi Protein Gels (Life Technologies). Membrane imaging was conducted with fluorescent secondary antibodies and a LI-COR Odyssey.

2.13. Statistical Analysis

Statistical analysis of western blot data was performed using GraphPadPrism software. One way ANOVA analysis followed by Dunnett's post-test was applied to datasets. A t-test was used to compare the mean of two groups of data. T tests were unpaired, two tailed with 95% confidence intervals.

3. Results

3.1. Exome Sequencing in familial ALS detects 16 protein-changing *TBK1* variants

We exome sequenced 699 index cases from a cohort of fALS from eleven countries, negative for mutations in all known ALS genes (including *SOD1*, *TDP43*, *C9ORF72*, *FUS*, *PFN1*, *UBQLN2*, *OPTN*, *VCP*, and *ANG*), and the intronic *C9ORF72* repeat expansion.

We identified 16 potentially deleterious protein-changing variants in *TBK1*, which were novel, or had an ExAC Non-Finnish European (NFE) carrier frequency of <1:20,000 individuals. A similar filtering strategy applied to the NFE subset of ExAC identified 54 variants from a total of 33,075 individuals, revealing a significant overabundance of protein-changing *TBK1* variants in our familiar cohort ($p=1.02e^{-10}$, Fisher's two-tailed test). Thirteen of these variants were absent from the following databases: 1000 genomes, UK10K, Exome Variant Server (EVS), and ExAC databases (n > 72,000). Two variants (p.R357Q, p.C471Y) were found once and one variant (p.R358H) was found seven times. Out of the 16 variants identified: four were nonsense, three in-frame deletion and nine were missense variants (Supplementary table 1). The p.G217R variant is present in two Dutch cases predicted to be first degree relatives (King kinship coefficient=0.314, vcftools Ajk=0.451), and is their only shared novel variant in a gene or pathway previously linked to ALS. The variant p.R357X is also present in a single FALS case in the ALS data browser (ALSdb) however, this is unlikely to be closely related to the p.R357X carrier identified in this study as they lack any other shared rare variants. Amongst the previously excluded FALS samples, another novel missense variant (p.Y394D) was identified in a patient who harbours the known pathogenic *TARDP* mutation, p.M337V, which segregated in their affected sibling. However, the available exome data did not have sufficient coverage to determine if the sibling also shared the *TBK1* variant and DNA was not available to determine segregation by Sanger sequencing. Furthermore, the *TBK1* variant p.R358H was present in both 1st-degree relatives of a kindred, but both were also carriers for the particularly aggressive *FUS* p.R521C mutation.

By mapping *TBK1* missense separately from nonsense variants we observed difference in their distribution (Figure1A,B). Whilst nonsense variants were spread across the whole protein, missense variants tended to cluster within the kinase domain (KD) and ubiquitin-like domain (ULD). Interestingly, the ULD has been reported to interact with both the scaffold dimerization domain (SDD) and the KD. These interactions play a vital role in the correct folding and dimerization of TBK1 (Li et al., 2012; Tu et al., 2013).

3.2. Selection of variants likely to be pathogenic

To focus our functional characterisation of *TBK1* variants identified in our cohort, we concentrated on three variants. We firstly chose the missense p.G217R variant as two related individuals carried this mutation and only one *TBK1* missense mutation had previously been shown to segregate with disease (van der Zee et al., 2017). The second nonsense variant p.R357X was selected as it was present in ALSdb. Three variants (p.G217R, p.R357X and p.C471Y) all scored highly using algorithms that predicted the variant to be damaging, and they appeared to be within functional domains according to the TBK1 homodimer crystal

structure (PDB 4IM0) (Figure 1C). The p.G217R mutation is located in the kinase domain and was predicted to be damaging by 17/20 of applied algorithms. The p.R357X mutation is located in the ULD and found to remove the entire SDD. The p.C471Y is located in the SDD and may therefore impair TBK1 homodimerisation (Figure 1 A,B).

3.3. ALS-linked *TBK1* variants decrease the phosphorylation of the TBK1 target IRF3

Some ALS and FTD associated *TBK1* variants have previously been shown to diminish or abolish phosphorylation of the TBK1 target IRF3 (Freischmidt et al., 2015; Kim et al., 2016; Pozzi et al., 2017; Tsai et al., 2016). In order to test the efficiency of p.G217R, p.R357X and p.C471Y on IRF3 phosphorylation, we transiently transfected HEK293T cells with wild-type (WT) or mutant *TBK1* and quantified IRF3 phosphorylation by Western blot. The expression levels of total IRF3 were comparable for WT and mutant constructs (Figure 2A,B), however, levels of phospho-IRF3 (pIRF3) were significantly reduced in p.G217R and p.R357X variant compared to the WT by western blot (Figure 2A,B) and immunocytochemistry (Figure 2D). Interestingly, the p.C471Y variant, predicted to be pathogenic by our bioinformatic tools, showed no difference from WT. Thus, both missense p.G217R and nonsense p.R357X mutations, but not the p.C471Y variant, abolished TBK1 kinase activity on its target IRF3.

3.4. ALS-linked *TBK1* variants decrease binding to OPTN and its phosphorylation

TBK1 is known to phosphorylate and regulate the activity of OPTN, a key receptor for poly-ubiquitinated proteins and mitochondria in autophagy pathways (Richter et al., 2016). TBK1 binds to the N-terminal region of OPTN (26–119) , via its C-terminal domain (residues 677–729) (Li et al., 2016) and phosphorylates it on Ser177 (Wild et al., 2011) and Ser473 (Heo et al., 2015; Richter et al., 2016). Since mutations in OPTN are also linked to ALS, we tested whether our ALS-associated *TBK1* variants affected its ability to bind to OPTN and phosphorylate it. Co-immunoprecipitation (Co-IP) of HA tagged WT and p.C471Y TBK1 consistently pulled down flag tagged OPTN (Figure 2C), however, p.G217R and p.R357X dramatically reduced TBK1 binding to OPTN. This finding was validated by the observation that the same two mutants also failed to phosphorylate OPTN. While TBK1 WT and p.C471Y generated a higher band on western blot that disappeared in the presence of alkaline phosphatase, the higher band is absent following co-transfection with OPTN WT and TBK1 p.G217R or p.R357X (Figure 2E). We conclude that both missense p.G217R and nonsense p.R357X mutations, but not p.C471Y, impair TBK1 binding to and phosphorylation of OPTN.

3.5. ALS-linked *TBK1* variants decrease the phosphorylation of TBK1

TBK1 is activated by the phosphorylation of Ser172, which causes a critical change in protein conformation promoting the active position of the C helix (Tu et al., 2013). We therefore tested whether the ALS-associated *TBK1* variants affect the phosphorylation and autophosphorylation of TBK1 itself. Western blots of HEK293T cells, transfected with each variant, were probed with an antibody specific for phospho-S172. Total TBK1 expression was similar for WT and all of the ALS-associated variants (Figure 3A,C). Robust levels of phospho-S172 TBK1 were evident in WT and p.C471Y transfected cells but were absent in cells expressing p.G217R and p.R357X (Figure 3A,B). Similarly, transfected HEK293T cells stained for phopsho-S172 TBK1 by immunocytochemistry confirmed that TBK1 phosphorylation was absent in cells expressing p.G217R and p.R357X mutants (Figure 3E). This indicates that the missense p.G217R and nonsense p.R357X but not the p.C471Y variant abolished the capacity of TBK1 for autophosphorylation.

3.6. ALS-linked variant p.G217R disrupts TBK1 homodimerisation

TBK1 has to homodimerise in order to be functional and does so via a central axis formed by aligning the two SDD domains in a parallel orientation. The ULD and KD domains interact with each other at one end of the dimer creating a globular structure and stabilising the homodimer (Tu et al., 2013) (Figure1C). We, therefore, investigated whether any of our variants affected the homodimerisation of TBK1 by transfecting HEK293T cells with TBK1 WT, p.G217R, p.R357X and p.C471Y and ran the lysates on non-denaturing gels (Figure 3B). Native blots revealed two strong high and low molecular weight bands for WT and p.C471Y TBK1, indicating that a similar proportion exists as a homodimer and monomer. Little dimerization, however, was evident for the p.G217R mutant and no band was visible for the p.R357X truncation mutant (Figure 3B,D). Quantification of the dimer/monomer ratio confirmed that the missense p.G217R kinase domain mutation showed a significantly lower TBK1 homodimerisation compared to WT ($p<0.05$) (Figure 3D).

3.7. TBK1 phosphorylation in ALS patient lymphoblastoid cell lines

In order to assess whether TBK1 activation is altered in ALS we measured total TBK1 and phospho-TBK1 in patient lymphoblastoid cell lines (LCLs) heterozygous for *TBK1* variants: p.T31A, c.992+1G>A (p.G272-T331del), p.R358H, p.Q565P, p.E643del and seven control LCLs. Firstly we sought to determine whether the c.992+1G>A causes an in-frame deletion of exon 8 within the ubiquitin-like domain. cDNA was amplified by PCR from the patient derived LCL harbouring the c.992+1G>A variant using primers flanking the whole of TBK1 and run an agarose gel (Supplementary Figure 1). We observed a lower band reflecting a ~200bp deletion, corresponding to the size of exon 8 and similar to the previously reported

c.992+1G<T (Gijselinck et al., 2015) and (c.992+4_992+7delAGTA) mutations (van der Zee et al., 2017). The skipping of exon 8 was confirmed by Sanger sequencing.

Quantification of western blots confirmed that total TBK1 was expressed at a similar level in all of the LCLs. Probing the same blots for phospho-S172-TBK1 revealed that the ratio between pTBK1 and total TBK1 is significantly different between patient and control derived LCLs (p=0.0229, Figure 4). Therefore, missense TBK1 mutations lead to reduced phosphorylation by self-interaction or with other kinases.

4. Discussion

In this study, we systematically analysed samples from 699 index fALS patients and identified 16 *TBK1* variants including 4 nonsense mutations, predicted to cause haploinsufficiency by nonsense mediated RNA decay or to be translated as truncated proteins. Three were in frame deletions and nine missense, which appear to cluster in the functional kinase and ubiquitin like domains known to play a role in TBK1 homodimerisation (Li et al., 2012; Tu et al., 2013). Five of these variants have never been published before: p.M623fs, p.Q629fs, p.T31A, p.R358H and c.992+1G>A (predicted to splice out the whole of exon 8 resulting in an in frame deletion within the ULD). The c.992+1G>A variant was reported once in ALSdb. Of the other variants only p.R357Q, p.E643del and p.T79del have been functionally investigated (Freischmidt et al., 2015; Gijselinck et al., 2015; van der Zee et al., 2017). Interestingly, disease onset in the patient harbouring both the *TBK1* p.Y394D and *TARDP* p.M337V mutations was 40 years (Table 1), which is 20 years earlier than the average age of onset described in literature (Pozzi et al., 2017). This double hit phenomenon was also described by Freischmidt and colleagues in the patients (all three affected relatives) harbouring *TBK1* p.Y185X and *FUS* p.R524G (Freischmidt et al., 2015).

We characterised the functional impact of three ALS-linked variants selected on the basis of their predicted disruption to key functional domains within TBK1 (Figure 1C). We chose p.G217R as it lies within the KD and was found in a putative affected sibling, p.R357X as it lies within the ULD and was found in an unrelated case in ALSdb and p.C471Y, which lies within the SDD. Only p.G217R and p.R357X *TBK1* variants, but not p.C471Y, abolished the phosphorylation of IRF3. This has previously been described for other ALS-associated mutations (Freischmidt et al., 2015; Kim et al., 2016; Tsai et al., 2016). The same *TBK1* variants, p.G217R and p.R357X, also abolished TBK1 binding to OPTN and prevented its phosphorylation. The inhibition of TBK1 binding to OPTN has been previously observed in ALS linked TBK1 variants, mainly located in the C-terminal region of the protein (Freischmidt et al., 2015; Kim et al., 2016; Pozzi et al., 2017; Tsai et al., 2016). However, the inhibition OPTN phosphorylation due to TBK1 mutations has never been shown before. A reduction in active OPTN phosphorylation would impair its

function as a receptor for polyubiquitinated proteins and result in the accumulation of TDP-43 which has been observed in patients harbouring *TBK1* mutations (Gijselinck et al., 2015; Pottier et al., 2015; van der Zee et al., 2017).

To become activated TBK1 must form a homodimer and be phosphorylated either by itself or by other kinases (Tu et al., 2013). Here we show that the p.G217R and p.R357X variants impair TBK1 autophosphorylation and its ability to be phosphorylated. This observation is consistent with a recent study that showed diminished TBK1 phosphorylation in ALS-associated *TBK1* in-frame deletions (p.T79del, p.D167del, p.E643del) (van der Zee et al., 2017). We have also shown that p.G217R, although located in the KD, affects TBK1 ability to homodimerise. In contrast, the p.C471Y variant within the SDD is able to phosphorylate and homodimerise at equivalent levels to the wildtype TBK1 protein and shows no evidence of pathogenicity.

Lastly, we demonstrated that there is a significant difference between phospho-TBK1 and total TBK1 ratio in patient compared to control derived LCLs. This supports the hypothesis that disease-linked TBK1 variants might impair TBK1 autophosphorylation, disrupting its ability to bind and phosphorylate multiple partners including OPTN.

5. Conclusions

We have identified four novel and 12 previously described *TBK1* variants in ALS patients. Our functional studies demonstrated that the missense mutation p.G217R in the KD has an almost identical profile as the truncation p.R357X in the ULD, and dramatically impairs the ability of TBK1 to form homodimers, auto-phosphorylate and function as a kinase. Furthermore, the proportion of TBK1 that is activated is significantly reduces in five lymphoblast ALS patient lines carrying missense or in-frame deletion mutations. Thus, missense mutations in critical functional domains may cause disease through a loss of TBK1 function supporting functional haploinsufficiency as a common TBK1 disease mechanism (Cirulli et al., 2015; Freischmidt et al., 2016, 2015). Further investigation of how ALS-linked *TBK1* variants alter TBK1 structure, phosphorylation and dimerisation will help unravel the disease pathogenesis and identify novel therapeutic targets.

6. Acknowledgement

We would like to thank people with motor neurone disease (MND) and their families for their participation in this project.

7. Disclosure statement

The authors have no actual or potential conflicts of interest.

8. Funding

This work was supported by Heaton-Ellis Trust, Motor Neurone Disease Association, Medical Research Council, the Wellcome Trust, the Noreen Murray Foundation, the American ALS Association and Project MinE. This is an EU Joint Programme - Neurodegenerative Disease Research (JPND) project. The project is supported through the following funding organisations under the aegis of JPND - www.jpnd.eu (United Kingdom, Medical Research Council and Economic and Social Research Council) and Horizon 2020 Programme (H2020-PHC-2014-two-stage; grant agreement number 633413). Bradley N Smith is supported by a Medical Research Fund Fellowship. CES and AAC receive salary support from the National Institute for Health Research (NIHR) Dementia Biomedical Research Unit at South London and Maudsley NHS Foundation Trust and King's College London. Samples used in this research were in part obtained from the UK National DNA Bank for MND Research, funded by the MND Association and the Wellcome Trust. Funding was provided to J.E.L. by the National Institutes of Health (NIH)/National Institute of Neurological Disorders and Stroke (NINDS) (R01NS073873) and the American ALS Association.

9. References

Brooks, B.R., Miller, R.G., Swash, M., Munsat, T.L., 2000. El Escorial revisited: Revised criteria for the diagnosis of amyotrophic lateral sclerosis. Amyotroph. Lateral Scler. Other Mot. Neuron Disord. 1, 293–299. https://doi.org/10.1080/146608200300079536

Cirulli, E.T., Lasseigne, B.N., Petrovski, S., Sapp, P.C., Dion, P.A., Leblond, C.S., Couthouis, J., Lu, Y.-F., Wang, Q., Krueger, B.J., Ren, Z., Keebler, J., Han, Y., Levy, S.E., Boone, B.E., Wimbish, J.R., Waite, L.L., Jones, A.L., Carulli, J.P., Day-Williams, A.G., Staropoli, J.F., Xin, W.W., Chesi, A., Raphael, A.R., McKenna-Yasek, D., Cady, J., Vianney de Jong, J.M.B., Kenna, K.P., Smith, B.N., Topp, S., Miller, J., Gkazi, A., FALS Sequencing Consortium, Al-Chalabi, A., van den Berg, L.H., Veldink, J., Silani, V., Ticozzi, N., Shaw, C.E., Baloh, R.H., Appel, S., Simpson, E., Lagier-Tourenne, C., Pulst, S.M., Gibson, S., Trojanowski, J.Q., Elman, L., McCluskey, L., Grossman, M., Shneider, N.A., Chung, W.K., Ravits, J.M., Glass, J.D., Sims, K.B., Van Deerlin, V.M., Maniatis, T., Hayes, S.D., Ordureau, A., Swarup, S., Landers, J., Baas, F., Allen, A.S., Bedlack, R.S., Harper, J.W., Gitler, A.D., Rouleau, G.A., Brown, R., Harms, M.B., Cooper, G.M., Harris, T., Myers, R.M., Goldstein, D.B., 2015. Exome sequencing in amyotrophic lateral sclerosis identifies risk genes and pathways. Science (80-.). 347, 1436–41. https://doi.org/10.1126/science.aaa3650

Freischmidt, A., Müller, K., Ludolph, A.C., Weishaupt, J.H., Andersen, P.M., 2016. Association of

Mutations in TBK1 With Sporadic and Familial Amyotrophic Lateral Sclerosis and Frontotemporal Dementia. JAMA Neurol. 74, 110. https://doi.org/10.1001/jamaneurol.2016.3712

Freischmidt, A., Wieland, T., Richter, B., Ruf, W., Schaeffer, V., Müller, K., Marroquin, N., Nordin, F., Hübers, A., Weydt, P., Pinto, S., Press, R., Millecamps, S., Molko, N., Bernard, E., Desnuelle, C., Soriani, M.-H., Dorst, J., Graf, E., Nordström, U., Feiler, M.S., Putz, S., Boeckers, T.M., Meyer, T., Winkler, A.S., Winkelman, J., de Carvalho, M., Thal, D.R., Otto, M., Brännström, T., Volk, A.E., Kursula, P., Danzer, K.M., Lichtner, P., Dikic, I., Meitinger, T., Ludolph, A.C., Strom, T.M., Andersen, P.M., Weishaupt, J.H., 2015. Haploinsufficiency of TBK1 causes familial ALS and fronto-temporal dementia. Nat. Neurosci. 1. https://doi.org/10.1038/nn.4000

Gijselinck, I., Van Mossevelde, S., Van Der Zee, J., Sieben, A., Philtjens, S., Heeman, B., Engelborghs, S., Vandenbulcke, M., De Baets, G., B??umer, V., Cuijt, I., Van Den Broeck, M., Peeters, K., Mattheijssens, M., Rousseau, F., Vandenberghe, R., De Jonghe, P., Cras, P., De Deyn, P.P., Martin, J.J., Cruts, M., Van Broeckhoven, C., 2015. Loss of TBK1 is a frequent cause of frontotemporal dementia in a Belgian cohort. Neurology 85, 2116–2125. https://doi.org/10.1212/WNL.0000000000002220

Heo, J.-M.M., Ordureau, A., Paulo, J.A.A., Rinehart, J., Harper, J.W.W., 2015. The PINK1-PARKIN Mitochondrial Ubiquitylation Pathway Drives a Program of OPTN/NDP52 Recruitment and TBK1 Activation to Promote Mitophagy. Mol. Cell 60, 1–14. https://doi.org/10.1016/j.molcel.2015.08.016

Jian, X., Boerwinkle, E., Liu, X., 2014. In silico prediction of splice-altering single nucleotide variants in the human genome. Nucleic Acids Res. 42, 13534–13544. https://doi.org/10.1093/nar/gku1206

Kim, Y.-E., Oh, K.-W., Noh, M.-Y., Nahm, M., Park, J., Lim, S.M., Jang, J.-H., Cho, E.-H., Ki, C.-S., Lee, S., Kim, S.H., 2016. Genetic and functional analysis of TBK1 variants in Korean patients with sporadic amyotrophic lateral sclerosis. Neurobiol. Aging 1–6. https://doi.org/10.1016/j.neurobiolaging.2016.11.003

Li, F., Xie, X., Wang, Y., Liu, J., Cheng, X., Guo, Y., Gong, Y., Hu, S., Pan, L., 2016. Structural insights into the interaction and disease mechanism of neurodegenerative disease-associated optineurin and TBK1 proteins. Nat. Commun. 7, 12708. https://doi.org/10.1038/ncomms12708

Li, J., Li, J., Miyahira, A., Sun, J., Liu, Y., Cheng, G., Liang, H., 2012. Crystal structure of the ubiquitin-like domain of human TBK1. Protein Cell 3, 383–391. https://doi.org/10.1007/s13238-012-2929-1

Ma, X., Helgason, E., Phung, Q.T., Quan, C.L., Iyer, R.S., Lee, M.W., Bowman, K.K., Starovasnik, M. a., Dueber, E.C., 2012. Molecular basis of Tank-binding kinase 1 activation by transautophosphorylation. Proc. Natl. Acad. Sci. 109, 9378–9383.

https://doi.org/10.1073/pnas.1121552109

Manichaikul, A., Mychaleckyj, J.C., Rich, S.S., Daly, K., Sale, M., Chen, W.M., 2010. Robust relationship inference in genome-wide association studies. Bioinformatics 26, 2867–2873. https://doi.org/10.1093/bioinformatics/btq559

Morgan, S., Orrell, R.W., 2016. Pathogenesis of amyotrophic lateral sclerosis. Br. Med. Bull. 119, 87–97. https://doi.org/10.1093/bmb/ldw026

Pottier, C., Bieniek, K.F., Finch, N., van de Vorst, M., Baker, M., Perkersen, R., Brown, P., Ravenscroft, T., van Blitterswijk, M., Nicholson, A.M., DeTure, M., Knopman, D.S., Josephs, K. a., Parisi, J.E., Petersen, R.C., Boylan, K.B., Boeve, B.F., Graff-Radford, N.R., Veltman, J. a., Gilissen, C., Murray, M.E., Dickson, D.W., Rademakers, R., 2015. Whole-genome sequencing reveals important role for TBK1 and OPTN mutations in frontotemporal lobar degeneration without motor neuron disease. Acta Neuropathol. 130, 77–92. https://doi.org/10.1007/s00401-015-1436-x

Pozzi, L., Valenza, F., Mosca, L., Dal Mas, A., Domi, T., Romano, A., Tarlarini, C., Falzone, Y.M., Tremolizzo, L., Sorarù, G., Cerri, F., Ferraro, P.M., Basaia, S., Agosta, F., Fazio, R., Comola, M., Comi, G., Ferrari, M., Quattrini, A., Lunetta, C., Penco, S., Bonanomi, D., Carrera, P., Riva, N., 2017. TBK1 mutations in Italian patients with amyotrophic lateral sclerosis: genetic and functional characterisation. J. Neurol. Neurosurg. Psychiatry 31, jnnp-2017-316174. https://doi.org/10.1136/jnnp-2017-316174

Richter, B., Sliter, D.A., Herhaus, L., Stolz, A., Wang, C., Beli, P., Zaffagnini, G., Wild, P., Martens, S., Wagner, S.A., Youle, R.J., Dikic, I., 2016. Phosphorylation of OPTN by TBK1 enhances its binding to Ub chains and promotes selective autophagy of damaged mitochondria. Proc. Natl. Acad. Sci. U. S. A. 113, 4039–4044. https://doi.org/10.1073/pnas.1523926113

Schindelin, J., Arganda-Carreras, I., Frise, E., Kaynig, V., Longair, M., Pietzsch, T., Preibisch, S., Rueden, C., Saalfeld, S., Schmid, B., Tinevez, J.-Y., White, D.J., Hartenstein, V., Eliceiri, K., Tomancak, P., Cardona, A., 2012. Fiji: an open-source platform for biological-image analysis. Nat. Methods 9, 676–82. https://doi.org/10.1038/nmeth.2019

Scotter, E.L., Vance, C., Nishimura, A.L., Lee, Y.-B.Y., Chen, H.H.-J., Urwin, H., Sardone, V., Mitchell, J.C., Rogelj, B., Rubinsztein, D.C., Shaw, C.E., 2014. Differential roles of the ubiquitin proteasome system and autophagy in the clearance of soluble and aggregated TDP-43 species. J. Cell Sci. 127, 1263–1278. https://doi.org/10.1242/jcs.140087

Taylor, P., Brown, R.H., Cleveland, D.W., 2016. Decoding ALS: from genes to mechanism. Nature 539, 197–206. https://doi.org/10.1038/nature20413

Tiwari, A., Xu, Z., Hayward, L.J., 2005. Aberrantly increased hydrophobicity shared by mutants of Cu,Zn-superoxide dismutase in familial amyotrophic lateral sclerosis. J. Biol. Chem. 280, 29771–29779. https://doi.org/10.1074/jbc.M504039200

Tsai, P.-C., Liu, Y.-C., Lin, K.-P., Liu, Y.-T., Liao, Y.-C., Hsiao, C.-T., Soong, B.-W., Yip, P.-K., Lee, Y.-C., 2016. Mutational analysis of TBK1 in Taiwanese patients with amyotrophic lateral sclerosis. Neurobiol. Aging 40, 191.e11-191.e16. https://doi.org/10.1016/j.neurobiolaging.2015.12.022

Tu, D., Zhu, Z., Zhou, A.Y., Yun, C. hong, Lee, K.E., Toms, A. V., Li, Y., Dunn, G.P., Chan, E., Thai, T., Yang, S., Ficarro, S.B., Marto, J. a., Jeon, H., Hahn, W.C., Barbie, D.A., Eck, M.J., 2013. Structure and Ubiquitination-Dependent Activation of TANK-Binding Kinase 1. Cell Rep. 3, 747–758. https://doi.org/10.1016/j.celrep.2013.01.033

van der Zee, J., Gijselinck, I., Van Mossevelde, S., Perrone, F., Dillen, L., Heeman, B., Bäumer, V., Engelborghs, S., De Bleecker, J., Baets, J., Gelpi, E., Rojas-García, R., Clarimón, J., Lleó, A., Diehl-Schmid, J., Alexopoulos, P., Perneczky, R., Synofzik, M., Just, J., Schöls, L., Graff, C., Thonberg, H., Borroni, B., Padovani, A., Jordanova, A., Sarafov, S., Tournev, I., de Mendonça, A., Miltenberger-Miltényi, G., Simões do Couto, F., Ramirez, A., Jessen, F., Heneka, M.T., Gómez-Tortosa, E., Danek, A., Cras, P., Vandenberghe, R., De Jonghe, P., De Deyn, P.P., Sleegers, K., Cruts, M., Van Broeckhoven, C., Goeman, J., Nuytten, D., Smets, K., Robberecht, W., Damme, P. Van, Bleecker, J. De, Santens, P., Dermaut, B., Versijpt, J., Michotte, A., Ivanoiu, A., Deryck, O., Bergmans, B., Delbeck, J., Bruyland, M., Willems, C., Salmon, E., Pastor, P., Ortega-Cubero, S., Benussi, L., Ghidoni, R., Binetti, G., Hernández, I., Boada, M., Ruiz, A., Sorbi, S., Nacmias, B., Bagnoli, S., Sorbi, S., Sanchez-Valle, R., Llado, A., Santana, I., Rosário Almeida, M., Frisoni, G.B., Maetzler, W., Matej, R., Fraidakis, M.J., Kovacs, G.G., Fabrizi, G.M., Testi, S., 2017. TBK1 Mutation Spectrum in an Extended European Patient Cohort with Frontotemporal Dementia and Amyotrophic Lateral Sclerosis. Hum. Mutat. 38, 297–309. https://doi.org/10.1002/humu.23161

Wang, K., Li, M., Hakonarson, H., 2010. ANNOVAR: Functional annotation of genetic variants from high-throughput sequencing data. Nucleic Acids Res. 38, 1–7. https://doi.org/10.1093/nar/gkq603

Weidberg, H., Elazar, Z., 2011. TBK1 Mediates Crosstalk Between the Innate Immune Response and Autophagy. Sci. Signal. 4, pe39-pe39. https://doi.org/10.1126/scisignal.2002355

Wild, P., Farhan, H., McEwan, D.G., Wagner, S., Rogov, V. V., Brady, N.R., Richter, B., Korac, J., Waidmann, O., Choudhary, C., Dotsch, V., Bumann, D., Dikic, I., Dötsch, V., Bumann, D., Dikic, I., Nakatogawa, H., Suzuki, K., Kamada, Y., Ohsumi, Y., Yang, Z., Klionsky, D.J., Levine, B., Mizushima, N., Virgin, H.W., Deretic, V., Kirkin, V., McEwan, D.G., Novak, I., Dikic, I., Kraft, C.,

Peter, M., Hofmann, K., McEwan, D.G., Dikic, I., Novak, I., Kirkin, V., Pankiv, S., Behrends, C., Sowa, M.E., Gygi, S.P., Harper, J.W., Wagner, S., Morton, S., Hesson, L., Peggie, M., Cohen, P., Clark, K., Plater, L., Peggie, M., Cohen, P., Radtke, A.L., Delbridge, L.M., Balachandran, S., Barber, G.N., O'Riordan, M.X., Thurston, T.L., Ryzhakov, G., Bloor, S., Muhlinen, N. von, Randow, F., Knodler, L.A., Perrin, A.J., Jiang, X., Birmingham, C.L., So, N.S., Brumell, J.H., Beuzón, C.R., Zheng, Y.T., Cemma, M., Kim, P.K., Brumell, J.H., Stehmeier, P., Muller, S., Jiang, H., Cheng, D., Liu, W., Peng, J., Feng, J., Cherra, S.J., Ikeda, F., Crosetto, N., Dikic, I., 2011. Phosphorylation of the Autophagy Receptor Optineurin Restricts Salmonella Growth. Science (80-.). 333, 228–233. https://doi.org/10.1126/science.1205405

Yang, J., Benyamin, B., Mcevoy, B.P., Gordon, S., Henders, A.K., Dale, R., Madden, P.A., Heath, A.C., Martin, N.G., Montgomery, G.W., Goddard, M.E., Visscher, P.M., 2011. Common SNPs explain a large proportion of heritability for human height 42, 565–569. https://doi.org/10.1038/ng.608.Common

10. Figure legends

Figure 1. TBK1 mutations identified to date and their location in TBK1 structure. (A,B) Schematic representation of TBK1 protein structure (Tu et al., 2013) showing a map of nonsense (A) and missense (B) variants found in literature and in our cohort. For more details on the variants found in this study see Supplementary table 1. (KD = Kinase domain (pink), ULD = Ubiquitin like domain (purple), SDD = Scaffold dimerization domain CTD = C-terminal domain (green)). (C) TBK1 homodimer crystal structure (PDB 4IM0) mapping the mutations found in our study excluding premature stop codons and frameshift deletions.

Figure 2. TBK1 p.G217R and p.R357X impair IRF3 phosphorylation as well as TBK1 binding with OPTN and its phosphorylation. (A) Western blot analysis of IRF3 (left) and pIRF3 (right). (B left) Quantitative analysis of blot in (A) left showing a similar expression level of endogenous IRF3 in cells (n=3). (B right) Quantitative analysis of blot in (A) right showing a significant decrease of expression of endogenous pIRF3 in cells transfected with TBK1-p.G217R and p.R357X (n=3, analysed by One Way ANOVA followed by Dunnett's post test $p<0.0001$). (C) Qualitative immunocytochemistry of HEK293T transfected with TBK1-WT, p.G217R, p.R357X and probed for p-IRF3 confirming the result obtained by western blot analysis (scale bar = 50 µm). (D) Co-IP with HA-tag pull down (TBK1) showing no biding of OPTN in any of the mutated samples with the exception of p.C471Y (n=3). (E) HEK293T were transiently co-transfected with Flag-OPTN WT and HA-TBK1 WT, p.G217R, p.R357X or p.C471Y, treated with alkaline phosphatase and analysed by western blot showing lack of OPTN phosphorylation in all mutated samples a part from p.C471Y.

Figure 3. TBK1 p.G217R and p.R357X impair TBK1 phosphorylation and auto phosphorylation and might reduce TBK1 homodimerisation. (A) Western blot analysis of TBK1 expression levels (left) and pTBK1 (right) (B left) Quantitative analysis of blot in (A) left showing a similar expression level of TBK1 in cells (n=4). (B right) Quantitative analysis of blot in (A) right showing a significant decrease of expression of pTBK1 in p.G217R and p.R357X (n=4 analysed by One Way ANOVA followed by Dunnett's post test $p<0.0001$). (C) Immunocytochemistry of HEK293T transfected with TBK1-WT, p.G217R, p.R357X and probed for p-TBK1 confirming the result obtained by western blot analysis (Figure 3) (Scale bar = 10 µm). (D) Native gel showing dimer and monomer (indicated by black arrows) in TBK1-WT and TBK1-C471Y, weaker dimer and monomer in p.G217R sample and no dimer or monomer in

R357X sample. (E) Quantitative analysis of gel in (D) showing significant reduction in dimer formation for p.G217R (positive control on the right TBK1 WT treated with DTT, n=3, analysed by One Way ANOVA followed by Dunnett's post test $p<0.05$).

Figure 4. Patient-derived LCLs harbouring *TBK1* variants show reduced level of TBK1 phosphorylation. (A top) Western blot of control and patient-derived LCLs, harbouring five different TBK1 variants, showing the level of total TBK1 (A bottom) Western blot showing phopsho-TBK1 expression in patient and control derived lymphoblasts. (B) Dot plot showing a significant difference the ratio of phospho-TBK1 and total TBK1 between control and patient derived LCLs (analysed by unpaired t-test, two tailed $p=0.0229$).

Supplementary figure 1. TBK1 variant c.992+1G>A produces the in-frame deletion of exon 8. Agarose gel on cDNA extracted from WT and c.992+1G<A (p.G272-T331 del) LCLs showing two different sized bands for the WT allele and the mutated allele carrying c.992+1 G>A compared to the sample carrying both WT alleles (WT/C992+1G>A WT allele: 2190 bp, WT/C992+1G>A mutated allele: 1990bp, WT/WT: 2190bp). The boxes above and below show the sequencing of the WT/WT sample and the sequencing of the WT/c.992+1G>A sample, respectively.

11. Tables

Type Of Variant	Exon	Nucleotide Variation[a]	Residue Change	Number of cases	Control Frequency	Gender	Clinical Diagnosis	Site of Onset	Age of Onset (years)	Disease duration (months)	Reference
Nonsense Variants	2	c.4C>T	p.Gln2Ter	1	0/82,513	F	ALS	S	60	-	(Cirulli et al. 2015; Gijselinck et al. 2015)
	9	c.1069C>T	p.Arg357Ter	1{1}	0/82,519	F	ALS	UL	76	-	(Cirulli et al. 2015)
	18	c.1869_1875del	p.Met623IlefsdTer9	1	0/82,359	F	ALS	-	43	20.4	-
	18	c.1887_1890del	p.Gln629HisfsTer4	1	0/82,445	F	ALS	-	-	-	-
In Frame Deletions	4	c.236_238delCAA	p.Thr79del	1	0/82,314	M	ALS	R	67.8	7.3	(van der Zee *et al.*, 2016)
	-	992+1 G>A	p.Gly272_Thr331del	1{1}	0/80,635	M	ALS	-	46	24	-
	18	c.1928_1930delAAG	p.Glu643del	1{1}	0/82,323	M	ALS	UL	64	48	(Cirulli et al. 2015; Freischmidt et al. 2015; Gijselinck et al. 2015; van der Zee et al. 2016)
Missense Variants	2	c.64A>C	p.Asn22His	1{1}	0/82,490	F	ALS	-	49	12	(Cirulli et al. 2015)
	2	c.92A>G	p.Thr31Ala	1	0/80,639	M	ALS	-	-	-	-
	5	c.385A>G	p.Asn129Asp	1	0/82599	M	ALS	L	68	-	(Cirulli et al. 2015)
	6	c.649G>A	p.Gly217Arg	1 (1*)	0/82,595	M,M	ALS	-	-	-	(Cirulli et al. 2015)
	9	c.1070G>A	p.Arg357Gln	1 {1}	1/82,519	M	ALS	LL	50	94	(Freischmidt *et al.*, 2015; Pozzi *et al.*, 2017)
	9	c.1073G>A	p.Arg358His	1(1*)	7/82519	-	-	-	-	-	-
	9	c.1180T>G	p.Tyr394Asp	1{1#}	0/82,080	F	ALS	B	40	-	(Cirulli et al. 2015)
	12	c.1412G>A	p.Cys471Tyr	1	1/79,400	F	ALS	-	-	-	(Cirulli et al. 2015)
	15	c.1694A>C	p.Gln565Pro	1 {1}	0/75,603	F	ALS	UL	50	36	(Cirulli et al. 2015)

Table 1 – TBK1 mutations identified in ALS patients by this study and their clinical phenotype. [a] Mutation nomenclature as recommended by the Human Genome Variation society www.hgvs.org, utilising +1 as the A of the initiator Met codon, translation start site. (*) affected relative from the present cohort. Cases number=699. The number in brackets ({}) represent the cases reported in ALSdb (http://alsdb.org/index.jsp). {#} represents duplicated sample found in ALSdb. S=spinal, UL=Upper Limb, R=respiratory, L=limb, LL=Lower Limb, B=bulbar.

12. Abbreviation list

ALS	Amyotrophic Lateral Sclerosis
ALSdb	Amyotrophic Lateral Sclerosis data base
ANG	Angiogenin
C9ORF72	Chromosome 9 Open Reading Frame 72
CTD	C-terminal domain
EVS	Exome Variant Server
ExAC	Exome Aggregation Consortium
fALS	Familial Amyotrophic Lateral Sclerosis
FTD	Frontotemporal Dementia
FUS	Fused in Sarcoma
GWAS	Genome Wide Association Studies
IRF3	Interferon Regulatory Factor 3
JPND	Joint Programme – Neurodegenerative Disease Research
KD	Kinase Domain
LCL	Lymphoblastoid Cell Lines
MND	Motor Neurone Disease
NFE	Non-Finnish European
OPTN	Optineurin
PDB	Protein Data Bank
PFN1	Profilin 1
SDD	Scaffold Dimerisation Domain
SOD1	Superoxide Dismutase 1
TBK1	Tank Binding Kinase 1
TDP43	TAR DNA-binding protein 43
UBQLN2	Ubiquilin 2
ULD	Ubiquitin-Like Domain
WES	Whole Exome Sequencing
WGS	Whole Genome Sequencing

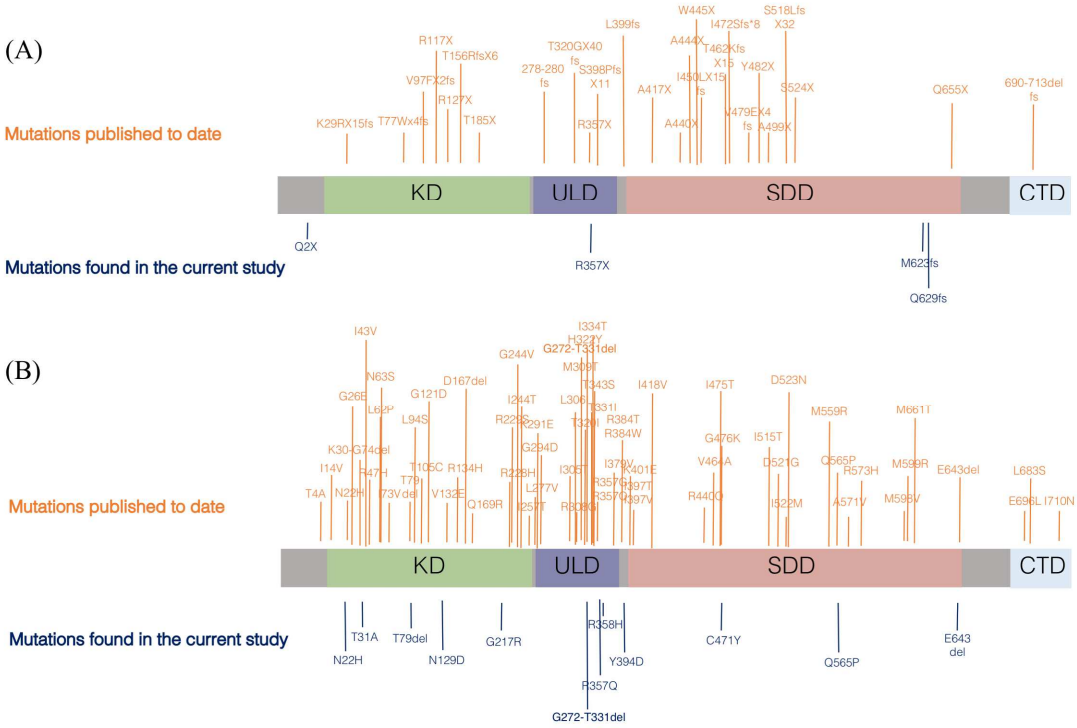
(A)
Mutations published to date
R117X
T156RfsX6
V97FX2fs
R127X
T185X
K29RX15fs
T77Wx4fs
278-280 fs
T320GX40 fs
S398Pfs X11
R357X
L399fs
A417X
W445X
A444X
I450LX15 fs
I472Sfs*8
T462Kfs
X15
Y482X
I479EX4 fs
A440X
A499X
S518Lfs X32
S524X
Q655X
690-713del fs
KD
ULD
SDD
CTD
Q2X
R357X
M623fs
Q629fs
Mutations found in the current study
(B)
Mutations published to date
I43V
N63S
G26E
L6P
G121D
D167del
K30-G74del
I14V
R47H
T4A
N22H
T79I
T73Vdel
T105C
R134H
V132E
Q169R
L94S
G244V
I334T
H327Y
G272-T331del
M309T
I244T
L306
R228S
R291E
G294D
R228H
L277V
H257T
T343S
T331I
R384T
R384W
I305T
I379V
R357Q
R357G
I397T
I397V
I418V
I475T
G476K
V464A
R440Q
D523N
I515T
D521G
I522M
M559R
Q565P
R573H
A571V
M661T
M599R
M599V
E643del
L683S
E696L I710N
KD
ULD
SDD
CTD
Mutations found in the current study
N22H
T31A
T79del
N129D
G217R
R358H
Y394D
R357Q
G272-T331del
C471Y
Q565P
E643 del

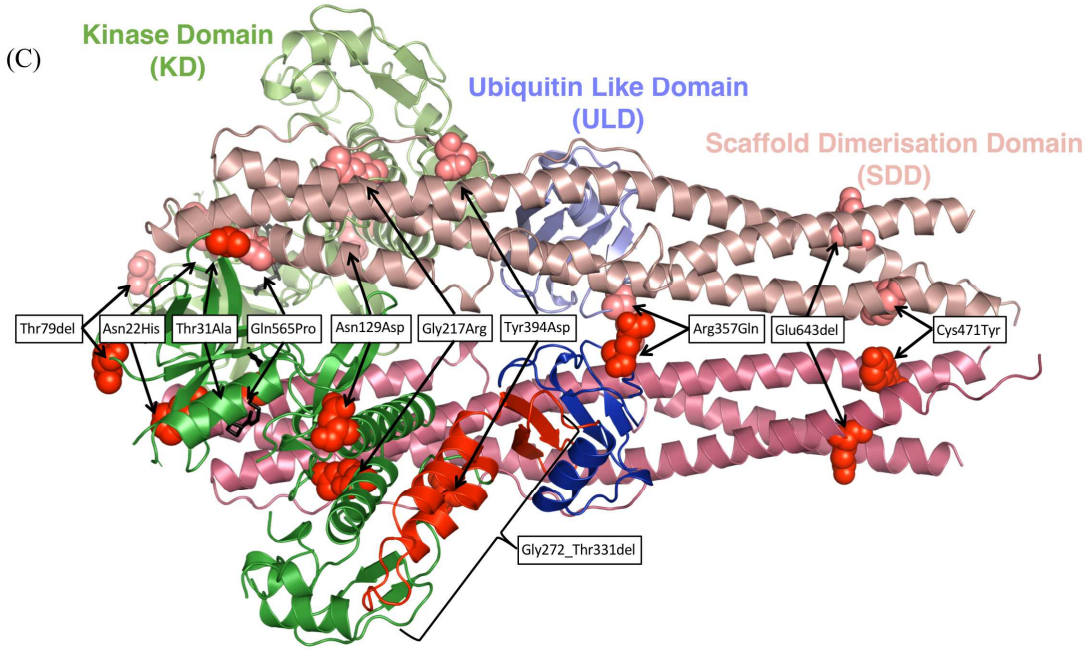
(C)
Kinase Domain (KD)
Ubiquitin Like Domain (ULD)
Scaffold Dimerisation Domain (SDD)
Thr79del
Asn22His
Thr31Ala
Gln565Pro
Asn129Asp
Gly217Arg
Tyr394Asp
Arg357Gln
Glu643del
Cys471Tyr
Gly272_Thr331del

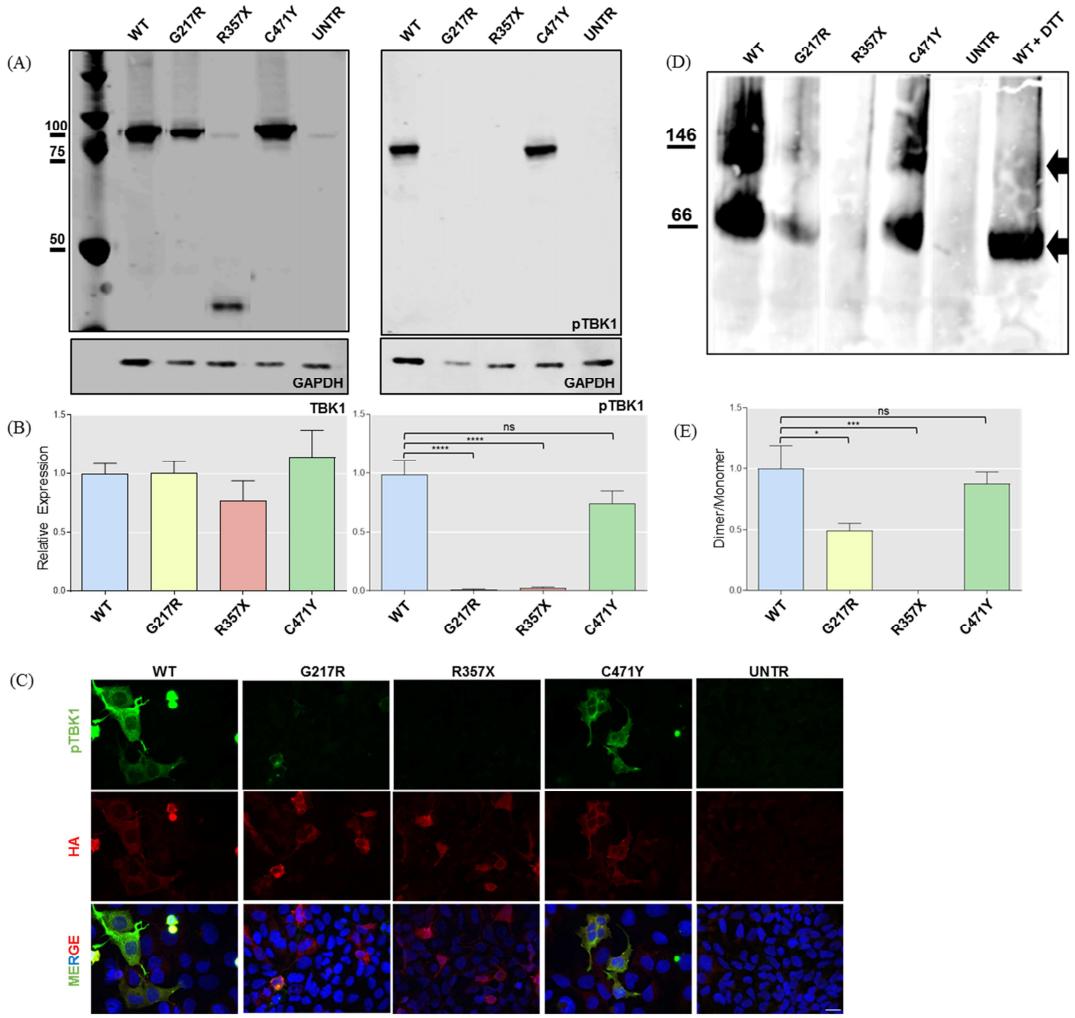
(A)
WT
G217R
R357X
C471Y
UNTR
100
75
50
pTBK1
GAPDH
(D)
WT + DTT
146
66
(B)
TBK1
pTBK1
Relative Expression
ns
(E)
Dimer/Monomer
(C)
pTBK1
HA
MERGE

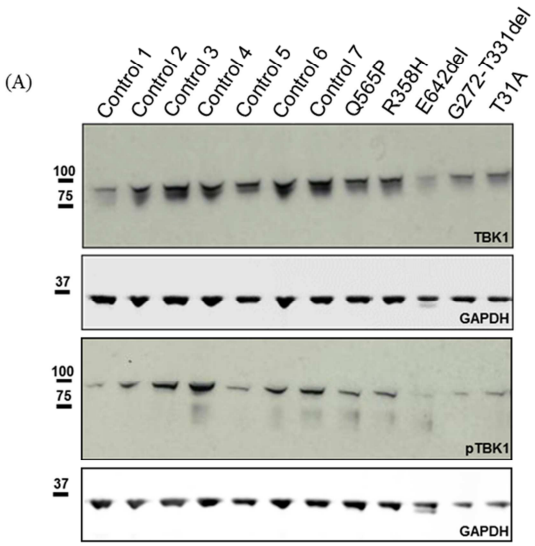

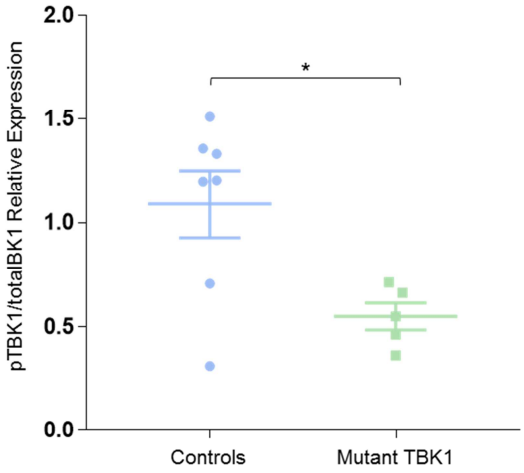

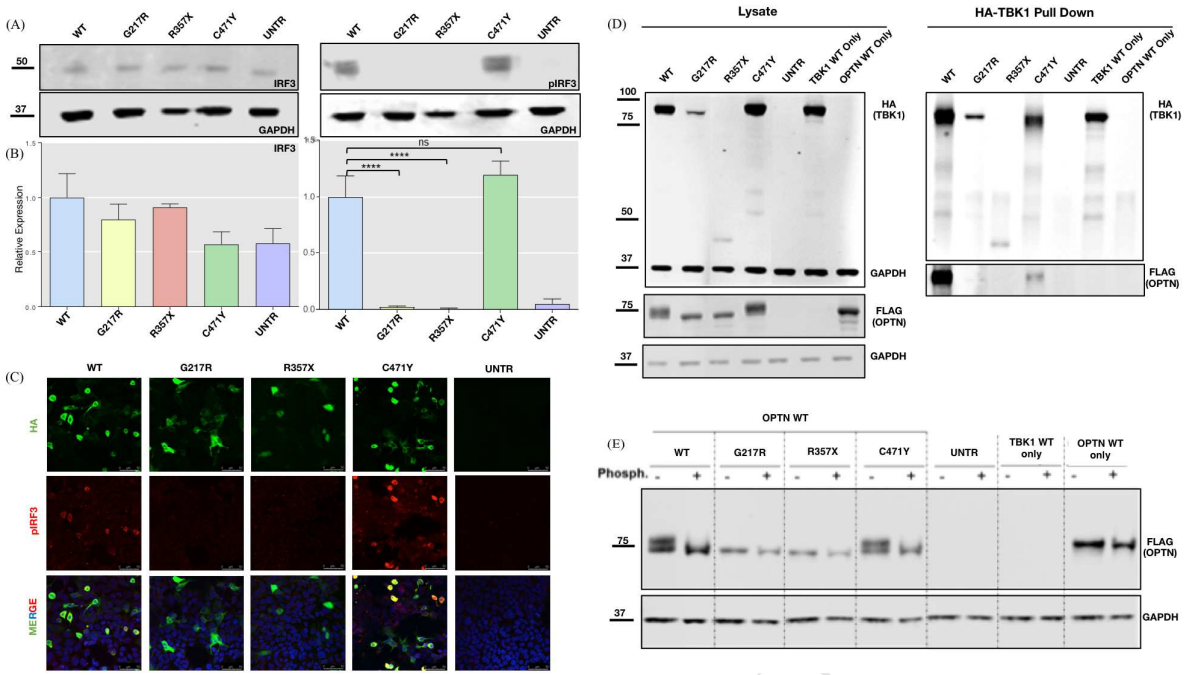

Highlights

- The p.R357X and p.G217R *TBK1* mutations both abolish TBK1 ability to phosphorylate two of its targets, IRF3 and optineurin (OPTN), to undergo phosphorylation as well as to bind OPTN.
- The proportion of active TBK1 (phosphorylated) is reduced in five lymphoblastoid cell lines derived from patients harbouring heterozygous missense or in-frame deletion *TBK1* mutations.
- Missense mutations in TBK1 functional domains impair the binding and phosphorylation of its normal targets, implicating a common loss of function mechanism, analogous to truncation mutations.